Computers and Geotechnics 70 (2015) 18–23

Contents lists available at ScienceDirect

Computers and Geotechnics

journal homepage: www.elsevier.com/locate/compgeo

Research Paper

An efficient remedy for the false volume expansion of DDA when simulating large rotation

W. Jiang [a,b], H. Zheng [a,*]

[a] State Key Laboratory of Geomechanics and Geotechnical Engineering, Institute of Rock and Soil Mechanics, Chinese Academy of Sciences, Wuhan 430071, China
[b] Collaborative Innovation Center for Geo-Hazards and Eco-Environment in Three Gorges Area, China Three Gorges University, Yichang 443002, China

ARTICLE INFO

Article history:
Received 5 December 2014
Received in revised form 16 July 2015
Accepted 18 July 2015
Available online 7 August 2015

Keywords:
Discontinuous deformation analysis (DDA)
Rigid body rotation
Volume expansion
Configuration update
Local frame

ABSTRACT

Although the constant strain mode of blocks assumed in the conventional discontinuous deformation analysis is sufficient for most applications in geotechnical engineering, a false volume expansion will occur in the presence of large block rotation. By introducing higher-order approximation to the displacements, the existing remedies can mitigate the false volume expansion to a limited extent; however, large acceleration variation or large rotation can still produce great errors. By fixing a local frame onto each block that moves and rotates with the block, the incremental strain components at the end of each time step are transformed to the local frame, which are then added to the total strain components with regard to the local frame. The false volume expansion is completely overcome with this method.

1. Introduction

After numerous verifications and enhancements, as described in Refs. [1,2], discontinuous deformation analysis (DDA) [3] is now recognized as an efficient tool for solving the various discontinuities in geotechnical problems. Because it is effective in simulating the dynamic mechanic behavior of block systems [4], DDA has been used to address diverse problems in various types of structures, such as the stability assessment of rock slopes [5]; the path tracking of rockfalls [6]; the blasting effect evaluation [7]; the simulation of landslides [8,9]; the construction of rock-fill dams [10], stacked block piles [11], and masonry structures [12]; and the analysis of coupled hydromechanical processes [13]. With the modification of the cohesion effect in sliding [14], DDA is expected to be used in the stability analysis of soil slopes.

With its extensive application in engineering, DDA has increasingly matured to solve problems that are more complicated. To obtain a more exact stress distribution, for example, the sub-block method [15] and higher-order displacement functions [16] have been introduced into DDA. Coupled with the finite element method (FEM) [17], the displacement precision of DDA has been improved. To simulate progressive failure, Jiang et al. introduced a viscous damping component to absorb the kinetic energy of discrete blocks [18]. To alleviate the sensibility of the penalty parameters, in addition to the Lagrange multiplier method [19], the complementarity method [20] and the variational inequality theory [21] have been successfully applied to reconfigure DDA without requiring penalty parameters. Recently, DDA has been reformulated as a linear complementarity problem [22], which further enhanced the convergence and solution efficiency.

The implementation of three-dimensional (3D) DDA is crucial to the analysis of practical problems. Many researchers have been devoted to this task. Since Shi [23] proposed a cutting procedure for 3D blocks, some contact algorithms and contact patterns have been suggested, such as the incision body method [24] and the common plane method [25]. Although all of these efforts improved 3D DDA, building a 3D program as robust as a two-dimensional (2D) program is still highly challenging. Recently, Shi published new contact theory [26], and it is believed that the difficulties in 3D DDA programming will be significantly simplified.

An unreasonable volume expansion is observed in the original DDA after the blocks undergo large rotation. This is considered to result from the errors accumulated by the first-order approximation of $\sin\theta \approx \theta$ and $\cos\theta \approx 1$. Here, θ is a small rotation angle. To restrain the false volume expansion, MacLaughlin and Sitar [27] adopted the second-order approximation of $\sin\theta$ and $\cos\theta$ to account for the effects of finite rotation. Ke [28] and Koo and Chern [30] proposed the use of a post-adjustment once the open–close iteration converges. By considering the trigonometric function transformations, Cheng and Zhang [29] introduced a new displacement variable and deformation matrix. To some

* Corresponding author. Tel.: +86 27 8719 9226; fax: +86 27 8719 7386.
E-mail address: hzheng@whrsm.ac.cn (H. Zheng).

http://dx.doi.org/10.1016/j.compgeo.2015.07.008
0266-352X/

degree, these remedies alleviated the false volume expansion due to large rotation; however, the best precision has not yet been achieved.

Because the incremental strain components at each time step, defined in the global frame, are not additive in the presence of finite rotation, a local frame is fixed onto each block, and the local frame is moved and rotated with the block. After the open–close iteration converges, the incremental strain components are transformed to the local frame, which are then added to the total strain components that are defined in the local frame. The displacement components at any point in the block can be accurately calculated through the displacement formula for finite rotation. As a result, no false volume expansion is observed, regardless of the degree of block rotation.

2. Review on the existing remedies for false volume expansion

On assuming a constant block strain mode, a typical block in the original DDA [1] is found to possess the following degrees of freedom vector:

$$\boldsymbol{d}^T = \begin{pmatrix} u_0 & v_0 & r_0 & \varepsilon_x & \varepsilon_y & \gamma_{xy} \end{pmatrix}, \tag{1}$$

where u_0 and v_0 represent the incremental displacement components of a reference point (x_0, y_0) of the block in the horizontal and vertical direction, respectively; r_0 is the incremental rigid rotation angle of the block around point (x_0, y_0); and $\varepsilon_x, \varepsilon_y$, and γ_{xy} are the incremental strain components based on the small deformation assumption.

Then, the incremental displacement vector at point (x, y) in this block is computed through

$$\boldsymbol{w} = \boldsymbol{T}\boldsymbol{d}, \tag{2}$$

with $\boldsymbol{T}$ being the 2×6 matrix,

$$\boldsymbol{T} = \begin{bmatrix} 1 & 0 & y_0 - y & x - x_0 & 0 & \frac{y-y_0}{2} \\ 0 & 1 & x - x_0 & 0 & y - y_0 & \frac{x-x_0}{2} \end{bmatrix}, \tag{3}$$

and $\boldsymbol{w}$ being the incremental displacement vector of point (x, y),

$$\boldsymbol{w}^T = (u, v). \tag{4}$$

Here, u and v are the incremental displacement components in the horizontal and vertical direction, respectively.

Once vector $\boldsymbol{d}$ is obtained through the open–close iteration, via DDA, it is added to the total degrees of freedom vector $\boldsymbol{d}^i$ of the last time step i by

$$\boldsymbol{d}^{i+1} = \boldsymbol{d}^i + \boldsymbol{d}, \tag{5}$$

with $\boldsymbol{d}^{i+1}$ being the total degrees of freedom vector of the current time step $(i + 1)$.

It is worth noting that Eq. (2) is derived by assuming a small deformation and a small rotation, where the following geometrical equations of small deformation are used:

$$\varepsilon_x = \frac{\partial u}{\partial x}, \quad \varepsilon_y = \frac{\partial v}{\partial y}, \text{ and } \gamma_{xy} = \frac{\partial u}{\partial y} + \frac{\partial v}{\partial x}, \tag{6}$$

and the first-order approximation to $\sin r_0$ and $\cos r_0$ results in

$$\sin r_0 \approx r_0 \text{ and } \cos r_0 \approx 1. \tag{7}$$

Because block displacement is mainly caused by its movement, and its deformation is usually small, assuming a small deformation will cause large errors even if the blocks are displaced to a great extent. In general, however, the total rotation cannot always be guaranteed to be small. If the block undergoes a large rotation, such as rock falling along slopes, its volume is greatly overestimated by the conventional DDA. This phenomenon is now referred to as false volume expansion. Several researchers have investigated solutions for this issue.

If only the small deformation is assumed, the displacement of a block is actually composed of two parts: the deformation of the block and the displacement due to rigid movement, leading to the displacement formula for finite rotation:

$$\begin{aligned} u &= u_0 + (x - x_0)(\cos r_0 - 1) - (y - y_0)\sin r_0 + (x - x_0)\varepsilon_x + \frac{y - y_0}{2}\gamma_{xy} \\ v &= v_0 + (x - x_0)\sin r_0 + (y - y_0)(\cos r_0 - 1) + (y - y_0)\varepsilon_y + \frac{x - x_0}{2}\gamma_{xy}. \end{aligned} \tag{8}$$

MacLaughlin and Sitar [27] noted that the first approximation to $\sin r_0$ and $\cos r_0$ resulted in an order of error by $0(r_0^3)$ and $0(r_0^2)$, respectively; therefore, the false volume expansion was mainly because $\cos r_0 \approx 1$ was assumed. As a result, they proposed representing the term $\cos r_0$ in Eq. (8) by $1 - r_0^2/2$, but keeping $\sin r_0 \approx r_0$. When Eq. (8) is directly applied, a stiffness matrix is produced with trigonometric functions that cannot be integrated easily; however, the procedure proposed by MacLaughlin and Sitar [27] still leads to the nonlinearity of this stiffness matrix, and the difficulties in convergence increase.

To avoid this issue, Ke [28] proposed that, after vector $\boldsymbol{d}$ is obtained through the open–close iteration, formula (8) can be used to obtain the incremental displacements u and v. Koo and Chern [30] also proposed a similar method. However, the error in each step accumulates so much so that the block is still noticeably distorted after undergoing a large rotation.

By means of the identity

$$\cos r_0 - 1 = -\sin^2 r_0/(1 + \cos r_0) \quad , \tag{9}$$

Cheng and Zhang [29] wrote Eq. (8) as the form

$$\boldsymbol{w} = \boldsymbol{T}'\boldsymbol{d}', \tag{10}$$

with

$$\boldsymbol{d}'^T = \begin{pmatrix} u_0 & v_0 & \sin r_0 & \varepsilon_x & \varepsilon_y & \gamma_{xy} \end{pmatrix}, \tag{11}$$

and

$$\boldsymbol{T}' = \begin{bmatrix} 1 & 0 & (x_0 - x)\frac{\sin r_0}{1+\cos r_0} - (y - y_0) & x - x_0 & 0 & \frac{y-y_0}{2} \\ 0 & 1 & (y_0 - y)\frac{\sin r_0}{1+\cos r_0} + (x - x_0) & 0 & y - y_0 & \frac{x-x_0}{2} \end{bmatrix}. \tag{12}$$

Because r_0 is unknown, Cheng and Zhang suggested taking r_0 in matrix $\boldsymbol{T}'$ as the value of the last time step. In fact, this implicitly assumes that all time steps are made equal and the angular acceleration is constant during the whole rotation.

3. New remedies for false volume expansion

Although some of the methods stated previously can alleviate false volume expansion, recently, all of them were observed to introduce large errors in the calculation of stresses, which are believed to result from the sum of the degrees of freedom vectors defined by Eq. (5). This can be explained as follows.

In the presence of finite rotation, the six components of vector $\boldsymbol{d}$ fall under two categories. The first two components, u_0 and v_0, represent the horizontal and vertical displacements with regard to the global coordinate system, and r_0 denotes the rigid rotation angle of the block. The three components have additivity regardless of the extent of block rotation. The latter three components, $\varepsilon_x, \varepsilon_y$, and γ_{xy}, are based on the small deformation assumption, and they do not have the property of additivity in the case of finite rotation. In fact, even if the differential element associated with

$\left(\varepsilon_x, \varepsilon_y, \gamma_{xy}\right)$ underwent a small rotation, the direct addition of incremental strain components would lead to a small but tangible error.

However, all DDA programs, conventional and improved, employ Eq. (5) to obtain the degrees of freedom vector $\boldsymbol{d}^{i+1}$ of the $(i+1)$-th step, implying

$$\varepsilon_x^{i+1} = \varepsilon_x^i + \varepsilon_x, \quad \varepsilon_y^{i+1} = \varepsilon_y^i + \varepsilon_y \quad \text{and} \quad \gamma_{xy}^{i+1} = \gamma_{xy}^i + \gamma_{xy}. \tag{13}$$

Most conventional DDA codes are updated in terms of stresses rather than strains. The update for stresses and strains is equivalent in the case of linear small deformation. If the material nonlinearity of blocks is considered, however, only strains can be added. The total stresses can be obtained only through the constitution integration over the total strains. This explains why strains rather than stresses are updated. When the approximations to block displacements are carried out in the framework of the numerical manifold method (NMM), the material nonlinearity of blocks is easy to implement. The structure of NMM codes is almost the same as DDA. The concept in this study can be applied to NMM.

The addition in Eq. (13) is always carried out in the global system, while the block is rotated by an angle of r_0^i after the i-th step is finished. Unless r_0^i is small enough, the accumulative error by Eq. (13) becomes very large even if the increment angle r_0 between any two consecutive time steps is small.

To overcome the false volume expansion and to correct the stress calculation, a local frame is fixed to each block at the reference point (x_0, y_0), as shown in Fig. 1. The two axes of the local frame are denoted by $\hat{x}$ and $\hat{y}$. At the start, axis-$\hat{x}$ and axis-$\hat{y}$ were parallel to the global axis-x and axis-y, respectively, as shown in the left side of Fig. 1; however, the local frame would later move and rotate with the block. For example, after the $(i+1)$-th step finished, the reference point (x_0, y_0) moved by the displacements

$$u_0^{i+1} = u_0^i + u_0 \text{ and } v_0^{i+1} = v_0^i + v_0, \tag{14}$$

and axis-$\hat{x}$ rotated to the orientation angle

$$r_0^{i+1} = r_0^i + r_0, \tag{15}$$

as shown in the right side of Fig. 1. In addition, the strain components could be additive only in the local frame, leading to

$$\hat{\varepsilon}_x^{i+1} = \hat{\varepsilon}_x^i + \hat{\varepsilon}_x, \quad \hat{\varepsilon}_y^{i+1} = \hat{\varepsilon}_y^i + \hat{\varepsilon}_y \text{ and } \hat{\gamma}_{xy}^{i+1} = \hat{\gamma}_{xy}^i + \hat{\gamma}_{xy}. \tag{16}$$

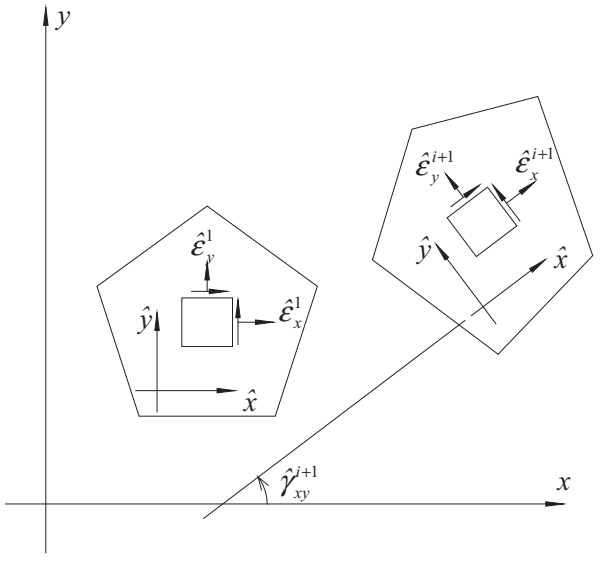

Fig. 1. Local frame attached to one block.

Here, the following notation convention is used: a variable with no cap, for example, u_0^{i+1}, is a variable under the global system, whereas a variable with a cap "∧", for example, $\hat{\varepsilon}_x^i$, is a variable under the local frame; a variable with a superscript, for example, u_0^i, is a variable at the i-th step, whereas a variable with no superscript, for example, $\hat{\gamma}_{xy}$, is an incremental variable. Therefore, $\hat{\varepsilon}_x, \hat{\varepsilon}_y$, and $\hat{\gamma}_{xy}$ in Eq. (16) are the incremental strain components in terms of the current local frame with axis-$\hat{x}$ making an angle of r_0^{i+1} with the global axis-x, as shown in the right side of Fig. 1. After the i-th increment finished, the incremental strain components, $\varepsilon_x, \varepsilon_y$ and γ_{xy}, calculated by DDA with regard to the global system need to be transformed into the local frame, leading to

$$\begin{aligned}
\hat{\varepsilon}_x &= \frac{\varepsilon_x + \varepsilon_y}{2} + \frac{\varepsilon_x - \varepsilon_y}{2}\cos 2r_0^{i+1} - \frac{1}{2}\gamma_{xy}\sin 2r_0^{i+1},\\
\hat{\varepsilon}_y &= \frac{\varepsilon_x + \varepsilon_y}{2} - \frac{\varepsilon_x - \varepsilon_y}{2}\cos 2r_0^{i+1} + \frac{1}{2}\gamma_{xy}\sin 2r_0^{i+1},\\
\hat{\gamma}_{xy} &= \left(\varepsilon_x - \varepsilon_y\right)\sin 2r_0^{i+1} + \gamma_{xy}\cos 2r_0^{i+1}.
\end{aligned} \tag{17}$$

Having obtained the total strain components $\hat{\varepsilon}_x^{i+1}, \hat{\varepsilon}_y^{i+1}$, and $\hat{\gamma}_{xy}^{i+1}$ in terms of the local frame via Eq. (16), the total strain components in terms of the global coordinate system are derived as follows:

$$\begin{aligned}
\varepsilon_x^{i+1} &= \frac{\hat{\varepsilon}_x^{i+1} + \hat{\varepsilon}_y^{i+1}}{2} + \frac{\hat{\varepsilon}_x^{i+1} - \hat{\varepsilon}_y^{i+1}}{2}\cos 2r_0^{i+1} + \frac{1}{2}\hat{\gamma}_{xy}^{i+1}\sin 2r_0^{i+1},\\
\varepsilon_y^{i+1} &= \frac{\hat{\varepsilon}_x^{i+1} + \hat{\varepsilon}_y^{i+1}}{2} - \frac{\hat{\varepsilon}_x^{i+1} - \hat{\varepsilon}_y^{i+1}}{2}\cos 2r_0^{i+1} - \frac{1}{2}\hat{\gamma}_{xy}^{i+1}\sin 2r_0^{i+1},\\
\gamma_{xy}^{i+1} &= \left(\hat{\varepsilon}_y^{i+1} - \hat{\varepsilon}_x^{i+1}\right)\sin 2r_0^{i+1} + \hat{\gamma}_{xy}^{i+1}\cos 2r_0^{i+1}.
\end{aligned} \tag{18}$$

The total displacements at point (x, y) of the block could be calculated by

$$\begin{aligned}
u =& u_0^{i+1} + (x - x_0)\left(\cos r_0^{i+1} - 1\right) - (y - y_0)\sin r_0^{i+1}\\
&+ (x - x_0)\varepsilon_x^{i+1} + \frac{y - y_0}{2}\gamma_{xy}^{i+1},\\
v =& v_0^{i+1} + (x - x_0)\sin r_0^{i+1} + (y - y_0)\left(\cos r_0^{i+1} - 1\right)\\
&+ (y - y_0)\varepsilon_y^{i+1} + \frac{x - x_0}{2}\gamma_{xy}^{i+1}.
\end{aligned} \tag{19}$$

The stress vector of the block at the $(i+1)$-th step is calculated by

$$\boldsymbol{\sigma}^{i+1} = \boldsymbol{E}\boldsymbol{\varepsilon}^{i+1}, \tag{20}$$

with $\boldsymbol{E}$ being the 3×3 elastic matrix and

$$\boldsymbol{\sigma}^{i+1} = \left(\sigma_x^{i+1}, \sigma_y^{i+1}, \tau_{xy}^{i+1}\right)^T \text{ and } \boldsymbol{\varepsilon}^{i+1} = \left(\varepsilon_x^{i+1}, \varepsilon_y^{i+1}, \gamma_{xy}^{i+1}\right)^T \tag{21}$$

representing the stress vector and the strain vector in the global system.

4. Implementation

Based on the above analysis, the false volume expansion in DDA is overcome by the following implementation:

(1) Through the open–close iteration, the incremental strain components, $\varepsilon_x, \varepsilon_y$, and γ_{xy}, in the global system are obtained.
(2) Using Eq. (15), the local frame orientation of the block at the end of this step is obtained.
(3) Using Eq. (17), the incremental strains, $\hat{\varepsilon}_x, \hat{\varepsilon}_y$, and $\hat{\gamma}_{xy}$, in terms of the local frame are obtained.
(4) Using Eq. (16), the total strains $\hat{\varepsilon}_x^{i+1}, \hat{\varepsilon}_y^{i+1}$, and $\hat{\gamma}_{xy}^{i+1}$, in terms of the local frame are obtained.
(5) Using Eqs. (18) and (20), the total strain vector $\boldsymbol{\varepsilon}^{i+1}$ and the total stress vector $\boldsymbol{\sigma}^{i+1}$ in the global system are obtained.

(6) Using

$$\ddot{u}_0 = \frac{2}{\Delta^2}u_0 - \frac{2}{\Delta}\dot{u}_0^i, \ldots,$$
$$\ddot{\hat{\varepsilon}}_x = \frac{2}{\Delta^2}\hat{\varepsilon}_x - \frac{2}{\Delta}\dot{\hat{\varepsilon}}_x^i, \ldots,$$

the accelerations within this step are calculated. Here, $\dot{u}_0^i$ is the initial horizontal speed at this step, $\dot{\hat{\varepsilon}}_x^i$ is the initial strain rate at this step, and Δ is the length of the time interval $[t^i, t^{i+1}]$.

(7) Using

$$\dot{u}_0^{i+1} = \dot{u}_0^i + \Delta\ddot{u}_0, \ldots,$$
$$\dot{\hat{\varepsilon}}_x^{i+1} = \dot{\hat{\varepsilon}}_x^i + \Delta\ddot{\hat{\varepsilon}}_x, \ldots,$$

the rates of change of these quantities at the end of this step are calculated.

(8) By replacing $\hat{\varepsilon}_x^{i+1}, \hat{\varepsilon}_y^{i+1}$, and $\hat{\gamma}_{xy}^{i+1}$ in Eq. (18) with $\dot{\hat{\varepsilon}}_x^{i+1}, \dot{\hat{\varepsilon}}_y^{i+1}$, and $\dot{\hat{\gamma}}_{xy}^{i+1}$, respectively, $\dot{\varepsilon}_x^{i+1}, \dot{\varepsilon}_y^{i+1}$, and $\dot{\gamma}_{xy}^{i+1}$ are calculated, which will contribute to the generalized force vector of this block in the next step.

(9) The rate vector $\boldsymbol{v}^{i+1}$, composed of $\dot{u}_0^{i+1}, \dot{v}_0^{i+1}, \dot{r}_0^{i+1}, \dot{\varepsilon}_x^{i+1}, \dot{\varepsilon}_y^{i+1}$, and $\dot{\gamma}_{xy}^{i+1}$, is regarded at the end of this step as the initial rate vector $\boldsymbol{v}_0$ of the next step, which contributes to the generalized force vector $\boldsymbol{q}$ of this block by

$$\frac{2}{\Delta'}\boldsymbol{M}\boldsymbol{v}^0 \rightarrow \boldsymbol{q},$$

with $\Delta' = t^{i+2} - t^{i+1}$,

$$\boldsymbol{M} = \int_\Omega \rho \boldsymbol{T}^T \boldsymbol{T} d\Omega,$$
$$\boldsymbol{v}^0 = \left(\dot{u}_0^{i+1}, \dot{v}_0^{i+1}, \dot{r}_0^{i+1}, \dot{\varepsilon}_x^{i+1}, \dot{\varepsilon}_y^{i+1}, \dot{\gamma}_{xy}^{i+1}\right)^T,$$
$$\boldsymbol{q} = \left(q_{u_0}, q_{v_0}, q_{r_0}, q_{\varepsilon_x}, q_{\varepsilon_y}, q_{\gamma_{xy}}\right)^T.$$

Here, q_{ε_x} is the dual force to the strain component, ε_x, etc. $\boldsymbol{\sigma}^{i+1}$ will be regarded as the initial stress $\boldsymbol{\sigma}^0$ of the block at the next step, which will contribute to the generalized forces as follows:

$$-S\sigma_x^{i+1} \rightarrow q_{\varepsilon_x}, -S\sigma_y^{i+1} \rightarrow q_{\varepsilon_y}, \text{ and } -S\tau_{xy}^{i+1} \rightarrow q_{\gamma_{xy}}.$$

Here, S is the area of the block.

5. Numerical examples

In this section, two typical examples are designed to demonstrate the effect of the proposed modification on the false volume expansion.

5.1. Rockfall problem

Rockfalls are a frequently occurring geologic hazard in mountain areas, which pose a threat to life and property. DDA is an efficient tool for analyzing this problem. To compare the effectiveness of different modifications in restraining the false block expansion, a rockfall problem is investigated, as shown in Fig. 2(a). The following parameters are used in the analysis: unit weight = 28 kN/m^3, Young's modulus = 2 GPa, and Poisson's ratio = 0.25. In this model, the slope is composed of fixed blocks, and the falling rock is a regular octagon with a unit diameter. The friction angle and cohesion strength between blocks are taken to be 0. Different time steps are considered in this problem, and the results are listed in Table 1. Fig. 2(b) displays the final configuration of the system.

For 2D problems discussed in this paper, the volume expansion of the rotating rock could be measured by its area. From Table 1, the area error of the original DDA is found to be markedly influenced by the time step: a longer time period results in a larger nonlinear block expansion. The Cheng and Zhang modification has a clear effect on the false expansion when the time step is kept constant, whereas the modification hardly adapts to the changing time step. The modifications proposed both in this study and by Ke have

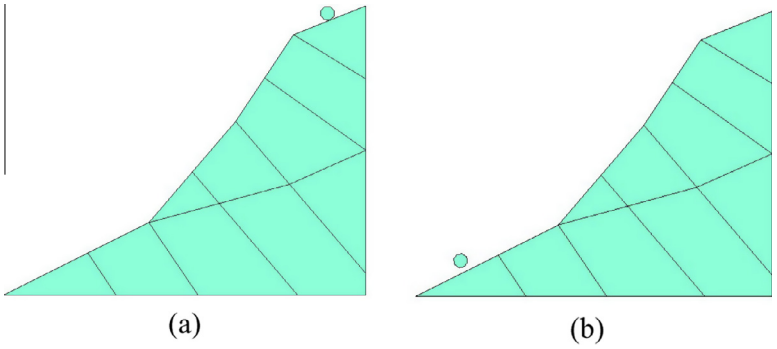

Fig. 2. Rockfall problems: (a) the initial state and (b) the final state.

Table 1
The area change of the falling rock by the original DDA, Ke's modification, the Cheng and Zhang modification, and the proposed modification.

Time-step △	0.01 s		0.02 s		0.01 s and 0.02 s alternately	
Steps	400		300		300	
Maximum displacement ratio per step	0.01		0.02		0.02	
Initial area of falling rock	0.707107 m^2					
	Area (m^2)	RE (%)	Area (m^2)	RE (%)	Area (m^2)	RE (%)
Original DDA	0.834560	18.025	1.264527	78.831	1.132795	60.201
Ke	0.707120	0.002	0.707114	0.001	0.707113	0.001
Cheng and Zhang	0.708365	0.178	0.731127	3.397	0.742573	5.016
Proposed	0.707119	0.002	0.707116	0.001	0.707119	0.002

*RE = Relative error.

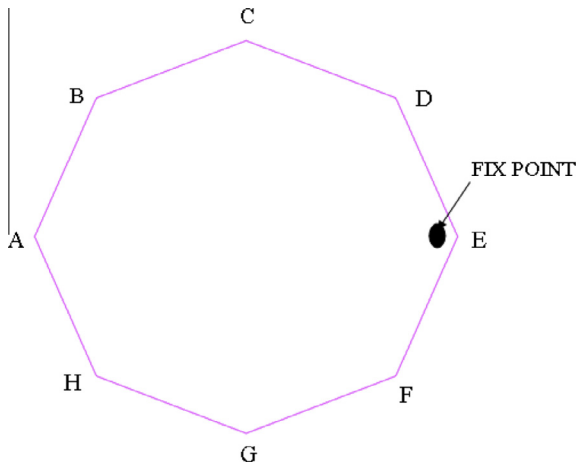

Fig. 3. A swing regular octagon fixed at an off-center point.

a clear effect on the false volume expansion, with the maximum relative error within 0.002% under different settings.

Therefore, the original DDA code must be modified to overcome the false volume expansion when simulating large rotation. Although the numerical errors in the Cheng and Zhang modification are larger than those in Ke's and the current study, all of them seem to be acceptable in engineering analysis. However, the accuracy of the accumulated strains of those modifications is still uncertain, and this problem is discussed in the next example.

5.2. Rotation of one regular octagon problem

Fig. 3 shows a single block fixed at an off-center point. In this problem, the block is a regular octagon with a diameter of 10. The coordinate of point A is (0, 0), and the coordinate of point E is (10, 0). The fixed point is at (9.5, 0.0). The block has the following material properties: unit weight = 28 kN/m^3, Young's modulus = 2 GPa, and Poisson's ratio = 0.25. Because this block is not fixed at its centroid, it will swing back and forth. By recording the length deformation of AE, BF, CG, and DH, we investigate whether the accumulated strains could be corrected by Ke's modification, the Cheng and Zhang modification, and the proposed modification.

Let the time step length Δ be 0.02 s, and let the maximum allowable step displacement ratio be 0.1. The data are recorded at steps of 200, 2000, and 5000. Table 2 lists the results from the three modifications.

The major principal strain and the minor principal strain correspond to the accumulated strains:

$$\varepsilon_{\max} = \frac{\varepsilon_x + \varepsilon_y}{2} + \sqrt{\left(\frac{\varepsilon_x - \varepsilon_y}{2}\right)^2 + \gamma_{xy}^2}$$
$$\varepsilon_{\min} = \frac{\varepsilon_x + \varepsilon_y}{2} - \sqrt{\left(\frac{\varepsilon_x - \varepsilon_y}{2}\right)^2 + \gamma_{xy}^2} \quad (22)$$

Table 3 lists the principal strains at different time steps computed by the three modifications. On analyzing the data in Tables 2 and 3, the principal strains by neither Ke's modification nor Cheng's modification are not in the interval of $[\varepsilon_{\min}, \varepsilon_{\max}]$ specified by Eq. (22).

Table 2
The length changes of four segments on the swing octagon in Fig. 3 by Ke's modification, the Cheng and Zhang modification, and the proposed modification.

Time steps		200		2000		5000	
		Length	Strain	Length	Strain	Length	Strain
Ke	AE	9.9969	−3.12E−04	10.0013	1.27E−04	10.0039	3.93E−04
	BF	10.0009	8.85E−05	10.0045	4.54E−04	10.0102	1.02E−03
	CG	10.0035	3.49E−04	9.9996	−3.83E−05	9.9962	−3.84E−04
	DH	9.9997	−2.68E−05	9.9965	−3.46E−04	9.9901	−9.89E−04
Cheng and Zhang	AE	9.9987	−1.29E−04	9.9984	−1.64E−04	10.006	5.99E−04
	BF	10.0025	2.50E−04	10.0039	3.88E−04	10.0129	1.29E−03
	CG	10.0052	5.17E−04	10.0052	5.24E−04	10.0089	8.88E−04
	DH	10.0015	1.53E−04	9.9999	−6.92E−06	10.0022	2.24E−04
Proposed	AE	9.9993	−6.57E−05	9.9998	−1.85E−05	10.0000	−3.60E−06
	BF	9.9994	−5.93E−05	10.0012	1.18E−04	10.0004	4.07E−05
	CG	10.0000	−7.43E−08	10.0009	8.75E−05	10.0002	1.61E−05
	DH	10.0001	1.24E−05	9.9997	−2.94E−05	9.9999	−9.97E−06

Table 3
Principal strains by Ke's modification, the Cheng and Zhang modification, and the proposed modification.

Time steps	ε_x	ε_y	γ_{xy}	$\varepsilon_{\max}$	$\varepsilon_{\min}$
Methods	*Ke*				
200	4.27 E−05	1.62E−05	−9.71E−05	1.27E−04	−6.86E−05
2000	8.02E−05	2.74E−05	1.72E−04	2.28E−04	−1.21E−04
5000	3.36E−05	−7.05E−06	2.31E−05	4.40E−05	−1.75E−05
Methods	*Cheng and Zhang*				
200	3.94E−05	1.84E−05	−9.68E−05	1.26E−04	−6.84E−05
2000	2.97E−06	2.95E−07	−2.85E−05	3.01E−05	−2.69E−05
5000	−2.83E−05	1.32E−04	6.42E−05	1.54E−04	−5.09E−05
Methods	*The proposed*				
200	4.49E−05	1.40E−05	−9.54E−05	1.26E−04	−6.73E−05
2000	8.35E−05	2.52E−05	1.72E−04	2.29E−04	−1.20E−04
5000	3.97E−05	−8.35E−06	2.56E−05	5.08E−05	−1.94E−05

Ke's modification can be taken as an example. The major principal strain at step-200 was 1.27×10^{-4} (see Table 3), which is less than the strain of line CG (3.49×10^{-4}) (see Table 2). The major strain at step-5000 is 4.40×10^{-5} in Table 3, which is less than the strain of line BF (1.02×10^{-3}) in Table 2 by up to two orders of magnitude. The same is true for the minor principal strain. The minor principal strain at step-200 is -6.86×10^{-5} in Table 3, which is lower in magnitude than the strain of line AE (-3.12×10^{-4}) in Table 2. The minor principal strain at step-5000 is -1.75×10^{-5} in Table 3, which is lower in magnitude than the strain of line DH (-9.89×10^{-4}) in Table 2.

The Cheng and Zhang modification has more serious limitations. For example, at step-200, the major principal strain is 1.26×10^{-4} (see Table 3), which is less than the strain of line CG (5.17×10^{-4}) (see Table 2). The minor principal strain is -6.84×10^{-5} in Table 3, which is lower in magnitude than the strain of line AE (-1.29×10^{-4}). At step-5000, the major principal strain is 1.54×10^{-4}, which is less than the strain of line BF (1.29×10^{-3}). Another serious limitation of the Cheng and Zhang modification is that the strain values of the four lines, AE, BF, CG, and DH, turn positive at step-500, which is clearly abnormal. As stated previously, the Cheng and Zhang modification holds only when the angular acceleration is kept invariant. However, the angular acceleration of the swing always varies - it accelerates as it rotates downward but decelerates as it rotates upward. This phenomenon explains why the Cheng and Zhang modification produces a large error while analyzing this example.

For all of the cases, all of the strain values of the four lines in Table 2 evaluated by the proposed modification are in the range of the principal strains in Table 3. Therefore, it is safe to state that the accumulated strain from the proposed modifications is the most reasonable.

6. Conclusions

By accumulating strains in the local frame of each block that moves and rotates with the block, the false volume expansion of blocks in DDA is effectively overcome even in the case of very large rotation or drastic variation in acceleration. The original DDA is not required to modify the deformation matrix $\boldsymbol{T}$ or the degree of freedom vector $\boldsymbol{d}$.

Acknowledgments

This study was supported by the National Basic Research Program of China (973 Program) under Grant Nos. 2011CB013505 and 2014CB047100 and the National Natural Science Foundation of China under Grant No. 11172313.

References

[1] MacLaughlin MM, Doolin DM. Review of validation of the discontinuous deformation analysis (DDA) method. Int J Numer Anal Meth Geomech 2006;30:271–305.
[2] Jing LR. Formulation of discontinuous deformation analysis (DDA) – an implicit discrete element model for block systems. Eng Geol 1998;49:371–81.
[3] Shi GH. Discontinuous deformation analysis: a new numerical model for the statics and dynamics of block systems, PhD Thesis. University of California, Berkeley; 1988.
[4] Ning YJ, Zhao ZY. A detailed investigation of block dynamic sliding by the discontinuous deformation analysis. Int J Numer Anal Meth Geomech 2011;37:2373–93.
[5] Hatzor YH, Arzi AA, Zaslavsky Y, Shapira A. Dynamic stability analysis of jointed rock slopes using the DDA method: King Herod's Palace, Masada, Israel. Int J Rock Mech Min Sci 2004;41:813–32.
[6] Cheng GQ. Numerical simulation in rockfall analysis: a close comparison of 2-D and 3-D DDA. Rock Mech Rock Eng 2013;46:527–41.
[7] Ning YJ, Yang J, Ma GW, Chen PW. Modeling rock blasting considering explosion gas penetration using discontinuous deformation analysis. Rock Mech Rock Eng 2011;44:483–90.
[8] Wu JH. Seismic landslide simulations in discontinuous deformation analysis. Comput Geotech 2010;37:594–601.
[9] Wu JH, Chen CH. Application of DDA to simulate characteristics of the Tsaoling landslide 2011;38:741–750.
[10] Kong XJ, Liu J. Dynamic failure numeric simulations of model concrete-faced rock-fill dam. Soil Dyn Earthquake Eng 2002;22:1131–4.
[11] Yagoda-Biran G, Hatzor YH. Constraining paleo PGA values by numerical analysis of overturned columns. Earthquake Eng Struct Dyn 2010;39:463–72.
[12] Kamai R, Hatzor YH. Numerical analysis of block stone displacements in ancient masonry structures: a new method to estimate historic ground motions. Int J Numer Anal Meth Geomech 2008;32:1321–40.
[13] Jing L, Ma Y, Fang Z. Modeling of fluid flow and solid deformation for fractured rocks with discontinuous deformation analysis (DDA) method. Int J Rock Mech Min Sci 2001;38:343–55.
[14] Wang L, Jiang H, Yang Z, Xu Y, Zhu X. Development of discontinuous deformation analysis with displacement-dependent interface shear strength. Comput Geotech 2013;47:91–101.
[15] Amadei B, Lin C, et al. Modeling fracture of rock masses with the DDA method. In: Nelson L, editor. Rock mechanics. Balkema; 1994. p. 583–90.
[16] Chern JC, Koo CY, Chen S. Development of second order displacement function for DDA and manifold method. In: Working forum on the manifold method of material analysis. Vicksburg; 1990. p. 183–202.
[17] Chang TC. Nonlinear dynamic discontinuous deformation analysis with finite element meshed block systems [D]. University of California at Berkeley; 1994.
[18] Jiang Q, Chen Y, Zhou C, Yeung MR. Kinetic energy dissipation and convergence criterion of Discontinuous Deformations Analysis (DDA) for geotechnical engineering. Rock Mech Rock Eng 2013;46:1443–60.
[19] Cai Y, Liang G, Shi GH. Studying impact problem by LDDA method. Discontinuous Deformation analysis (DDA) and simulations of discontinuous media. TSI Press; 1996.
[20] Zheng H, Jiang W. Discontinuous deformation analysis based on complementary theory. Sci China Ser E: Technol Sci 2009;52:2547–54.
[21] Jiang W, Zheng H. Discontinuous deformation analysis based on variational inequality theory. Int J Comput Methods 2011;8:193–208.
[22] Zheng H, Li XK. Mixed linear complementarity formulation of discontinuous deformation analysis. Int J Rock Mech Mining Sci 2015;75:23–32,.
[23] Shi GH. Producing joint polygons, cutting joint blocks and finding key blocks for general free surface surfaces. Chin J Rock Mech Eng 2006;25:2161–70.
[24] Wang JQ, Lin G. Static and dynamic stability analysis using 3D-DDA with incision body scheme. Earthquake Eng Eng Vib 2006;5:273–84.
[25] Liu J, Geng QD, Kong XJ. A fast common plane identification algorithm for 3D contact problems. Comput Geotech 2009;36:41–51.
[26] Shi GH. Contact theory. Sci China Technol Sci 2015;58:1–147.
[27] MacLaughlin MM, Sitar N. Rigid body rotations in DDA. In: Proceedings of the first international forum on Discontinuous Deformation Analysis (DDA) and simulations of discontinuous media. USA: TSI Press; 1996. p. 620–35.
[28] Ke TC. The issue of rigid-body rotation in DDA. In: Proceedings of the first international forum on Discontinuous Deformation Analysis (DDA) and simulations of discontinuous media. USA: TSI Press; 1996. p. 318–25.
[29] Cheng YM, Zhang YH. Rigid body rotation and block internal discretization in DDA analysis. Int J Numer Anal Meth Geomech 2000;24:567–78.
[30] Koo CY, Chern JC. Modification of the DDA method for rigid block problems. Int J Rock Mech Mining Sci 1998;35:683–93.